

Synthesis and Characterization of Germanium Coordination Compounds for Production of Germanium Nanomaterials

Timothy J. Boyle,^{*[a]} Louis J. Tribby,^[b] Leigh Anna M. Ottley,^[a] and Sang M. Han^[b]

Keywords: Germanium / Nanomaterials / Alkoxides / Thiols / Amides / Solid-state structures

A series of novel germanium(II) precursors was synthesized to initiate an investigation between the precursors' structures and the morphologies of the resulting nanoparticles. The precursors were synthesized from the reaction of $\text{Ge}[\text{N}(\text{SiMe}_3)_2]_2$ or $[\text{Ge}(\text{OtBu})_2]_2$ and the appropriate ligand: *N,N'*-dibenzylethylenediamine (H₂-DBED), *tert*-butyl alcohol (H-OtBu), 2,6-dimethylphenol (H-DMP), 2,6-diphenylphenol (H-DPP), *tert*-butyldimethylsilanol (H-DMBS), triphenylsilanol (H-TPS), triphenylsilanethiol (H-TPST), and benzenethiol (H-PS). The products were identified as: $[\text{Ge}(\mu\text{-DBED})]_2$ (**1**, $\mu\text{-c}$ = bridging chelating), $[\text{Ge}(\mu\text{-DMP})(\text{DMP})]_2$ (**2**), $\text{Ge}(\text{DPP})_2$ (**3**), $[\text{Ge}(\mu\text{-OtBu})(\text{DMBS})]_2$, (**4**), $[\text{Ge}(\mu\text{-DMBS})(\text{DMBS})]_2$ (**5**), $\text{Ge}(\text{TPS})_3(\text{H})$ (**6**), $[\text{Ge}(\mu\text{-TPST})(\text{TPST})]_2$ (**7**), and $\text{Ge}(\text{PS})_4$ (**8**).

The Ge^{II} metal centers were found to adopt a pyramidal geometry for **1**, **2**, **4**, **5**, **7**, a bent arrangement for **3**, and a tetrahedral coordination for the Ge^{IV} species **6** and **8**. Using a simple solution precipitation methodology, Ge⁰ nanomaterials were isolated as dots and wires for the majority of precursors. Compound **7** led to the isolation of amorphous Ge_xS_y. The nanomaterials isolated were characterized by TEM, EDS, and powder XRD. A correlation between the precursor's arrangement and final observed nanomorphology was proffered as part of the "precursor structure affect" phenomenon.

(© Wiley-VCH Verlag GmbH & Co. KGaA, 69451 Weinheim, Germany, 2009)

Introduction

Germanium has come to the forefront of a possible replacement material for silicon in such applications as transistors,^[1–3] nonvolatile memories,^[4–6] photovoltaic devices,^[7–9] long-wavelength photodetectors,^[10] and biological detection systems.^[11,12] This fundamental materials change is being explored since it is expected that Ge-based electronics will display:¹ enhanced electrical properties, owing to higher electron and hole mobility than noted for Si,^[13] (ii) smaller band gap behavior^[6] (even though bulk Ge is an indirect band gap material),^[14] and (iii) a more pronounced quantum confinement in comparison to Si due to the larger Bohr exciton radius of Ge.^[15–19] Unfortunately, further development of these devices has been hindered by the lack of a simple, rapid, high purity route to Ge nanomaterials.^[20,21]

Recently, we reported on the synthesis of Ge⁰ nano-dots and -wires from the decomposition of select Ge^{II} precursors (e.g., amide vs. alkoxide)^[21] that avoided the use of high temperatures, high pressures, seed catalysts, and retention of competing salt by-products reported for other literature

preparatory routes.^[22–36] For our method, Ge^{II} precursors were selected since the reduction potential of Ge^{II} to Ge⁰ is +0.247 V in comparison to the +0.124 V reported for Ge^{IV} to Ge⁰.^[37] Of particular note for this route was the fact that the ligand set of the precursor appeared to influence the final observed Ge⁰ morphology.^[21] This phenomenon was referred to as the "precursor structure affect" (PSA) and has been investigated and confirmed for a number of other systems.^[38–40]

In order to further probe the PSA for this system, a larger family of varied Ge^{II} precursors was necessary. However, a search of the literature^[41,42] revealed that only a handful of acceptable structurally characterized Ge^{II} precursors (i.e., amides, alcohols) for the production of Ge⁰ nanomaterials were available.^[21,43–71] Since both the steric bulk of the pendant chains of the alkoxide^[72] and the bond dissociation energies [Ge-N (55 kcal/mol),^[73] Ge-O (157),^[73] Ge-S (128)]^[74] of a the Ge^{II} precursors were shown to play a role in the PSA, the synthesis and characterization of series of Ge^{II} coordination compounds bound by a variety of ligands was warranted.

These compounds were generated through either the well-established transamination^[66–71] reaction [Equation (1)], where $\text{Ge}(\text{NR}_2)_2$ ($\text{R} = \text{SiMe}_3$)^[59,60,75] was substituted with a series of amines, alcohols, thiols (collectively referred to as H-L) or the often used alcoholysis exchange [Equation (2)] involving $[\text{Ge}(\text{OtBu})_2]_2$.^[47,76] The H-L modifiers investigated in this work included *N,N'*-dibenzylethylenediamine (H₂-DBED), *tert*-butyl alcohol (H-OtBu), 2,6-dimethyl-

[a] Sandia National Laboratories, Advanced Materials Laboratory, 1001 University Boulevard SE, Albuquerque, New Mexico 87106, USA
Fax: +1-505-272-7336
E-mail: tjboyle@sandia.gov

[b] Department of Nuclear and Chemical Engineering, 1 University of New Mexico, Albuquerque, NM 87131-0001, USA

Supporting information for this article is available on the WWW under <http://dx.doi.org/10.1002/ejic.200900556>.

phenol (H-DMP), 2,6-diphenylphenol (H-DPP), *tert*-butyldimethylsilanol (H-DMBS), triphenylsilanol (H-TPS), triphenylsulfanethiol (H-TPST), and benzenethiol (H-PS). The products were identified as: [Ge(μ_c -DBED)]₂ (**1**, μ_c = bridging chelating), [Ge(μ -DMP)(DMP)]₂ (**2**), Ge(DPP)₂ (**3**), [Ge(μ -*Or*Bu)(DMBS)]₂ (**4**), [Ge(μ -DMBS)(DMBS)]₂ (**5**), Ge(TPS)₃(H) (**6**), [Ge(μ -TPST)(TPST)]₂ (**7**), and Ge(PS)₄ (**8**). Once isolated, these compounds were used for the generation of Ge-based nanomaterials following established solution precipitation protocols.^[21] The characterization of these precursors, the nanomaterials produced and the preliminary PSA correlation are discussed.



H-L	Formula
H ₂ -DBED = <i>N,N'</i> -dibenzylethylenediamine	1 [Ge(μ_c -DBED)] ₂
H-DMP = 2,6-dimethylphenol	2 [Ge(μ -DMP)(DMP)] ₂
H-DPP = 2,6-diphenylphenol	3 Ge(DPP) ₂
H-DMBS = <i>tert</i> -butyldimethylsilanol	5 [Ge(μ -DMBS)(DMBS)] ₂
H-TPS = triphenylsilanol	6 Ge(TPS) ₃ (H)
H-TPST = triphenylsulfanethiol	7 [Ge(μ -TPST)(TPST)] ₂
H-PS = benzenethiol	8 Ge(PS) ₄



Results and Discussion

The utility of Ge^{II} amide [Ge(NR₂)₂] and alkoxide [Ge(OR)₂] derivatives for the production of Ge⁰ nanomaterials has been previously demonstrated.^[21] In an effort to garner additional morphological control over the Ge⁰ nanomaterials by exploiting the PSA phenomenon, a series of well-characterized Ge(NR₂)₂ and Ge(OR)₂ precursors was necessary. A search of the crystallographically characterized species^[41,42] constrained to Ge(NR₂)₂ yielded a complex family of compounds^[50,52–58] that typically employ chelating amide groups as well as a series of simple Ge[N(SiR₃)₂]₂^[59–62,75] species. Further searches for Ge(OR)₂ structures (when calixarenes and hydroxy ligated species were removed due to inherent problems associated with these compounds for materials production) yielded two structure types: (i) monomeric Ge(OR)₂ where OR = OC(*t*Bu)₃,^[49] O(CH₂)₂NMe₂,^[63] (2,6-di-R)phenoxy [R = *tert*-butyl (DBP),^[21] *tert*-butyl-Me-4,^[51] 2,6-isopropylphenyl,^[43] phenyl (DPP)],^[45] (2,3,5,6-tetraphenyl)phenoxy,^[45] Ge(DPP)₂(NMe₂)₂^[77] and (ii) dinuclear [(OR)Ge(μ -OR)]₂ where OR = mesityloxo (OMes)^[45] and 2,6-diisopropylphenoxy (DIP).^[45] Additionally, for Ge^{II} siloxides, the heteroligated [(TPS)Ge(μ -*Or*Bu)]₂^[47] and Ge(TPS)₂-{(TMS)N=P(PH)₂}(CH₂)₂^[64] have been disseminated as well as the Ge^{IV} bis-OSiR₃ complex (porph)Ge(TPS)₂ {porph = 5,10,15,20-tetrakis[(2-triisopropylsilyl)ethynyl]-porphyrinato-*N,N',N'',N'''*}.^[78] We were also interested in the utility of thiolate derivatives as precursors for Ge⁰ or single-source precursor for GeS_x. Only a handful of Ge^{II} thiolates have been crystallographically reported, including [Ge(μ -*St*Bu)₂(*St*Bu)]₂,^[79] the hydrido Ge(SPh₃)₃(H),^[45] and the salts [Ge(SPh₃)₃][N(Et)₄]^[65] or [(SCH₂CH₂S)^cGe(μ -SCH₂CH₂S)₂][P(Ph)₄] (^c stands for *cyclic*).^[65]

Obviously, the systematic variation and the proper ligand composition to investigate the PSA of Ge⁰ nanomaterials were not available from this set of compounds.^[21,38–40,43–65] Therefore, the syntheses of Ge^{II} precursors with ligands selected for both electronic and steric considerations were initiated. Once isolated and characterized, an initial study on the conversion of these precursors to Ge⁰ nanomaterials via a solution precipitation route was undertaken.^[21]

Synthesis

The ligands of interest [H-L, Equation (1)] were individually reacted with Ge(NR₂)₂^[59,60,75] in toluene [Equation (1)]; except for **4** which was isolated from the modification of [Ge(*Or*Bu)₂]₂^[47,76] [Equation (2)]. After stirring for 10 min, each reaction mixture was set aside and the volatile component was allowed to slowly evaporate. Over an extended period of time under an argon atmosphere, light yellow or colorless X-ray quality crystals were isolated. FTIR data of the dried crystals indicated that the reactive proton for each ligand had been removed. In particular, the H–N stretch for the diamine at ca. 3300 cm^{–1} for compound **1**, the H–O stretch of the alcohols at 3200–3500 cm^{–1} for **2**, **3** and for the silanols of **4–6**, as well as the H–S stretch for the thiols at ca. 2500 cm^{–1} for **7** and **8** were no longer present. For **6**, a new peak at 2130 cm^{–1} was tentatively assigned to a Ge–H stretching band.^[80–83] For **5**, a peak at 2131 cm^{–1} was observed which was tentatively assigned to a Ge–H interaction, possibly from the protons of the Si(CH₃)₃ group.

Crystal Structures

In order to assist in the characterization of **1–8**, single-crystal X-ray structures of each were obtained and shown in Figures 1, 2, 3, 4, 5, 6, 7, and 8, respectively. The structure plot of compound **1** (Figure 1) shows the structure of the Ge^{II} diamine derivative. For **1**, each pyramidal Ge metal center is fully coordinated by three N atoms – two from the chelating DBED and one from the N of the other DBED. The ethane linkage of each DBED was found to be twisted 24.3° out of the plane with respect to the core, which is in good agreement with the 22.0° twist of the monomeric [CH₂N(*t*Bu)]₂Ge.^[54] The remainder of comparable metrical data are also in agreement between **1** [Ge–N(1) 1.86 Å; N–Ge–N 84.6°] and [CH₂N(*t*Bu)]₂Ge [Ge–N 1.83 Å; N–Ge–N 87.9°].^[54] The Ge₂N₂ core of **1** [Ge(μ -N) av. 2.01 Å, (μ -N)–Ge(μ -N) 80.0°] compares favorably to [C₆H₃-2,6(C₆H₃-2,6-*i*Pr₂)₂(μ -NH₂)Ge]₂^[41] [Ge(μ -N) 2.02 Å; (μ -N)–Ge(μ -N) angle of 81.5°].

The use of aryl alcohols in Equation (1), led to the isolation of **2** (Figure 2) and **3** (Figure 3). For the smaller DMP ligand, the dinuclear compound **2** was isolated with a single bridging and terminal DMP ligand bound to each pyramidal coordinated Ge metal center. The terminal DMP ligands adopt a *trans* arrangement (above and below the Ge₂O₂ plane), similar to what was reported for the OMe^s^[45] and DIP^[45] derivatives. As is often noted for metal alk-

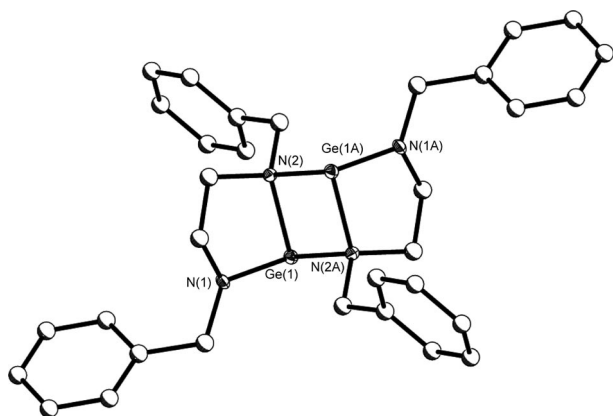


Figure 1. Structure plot of **1**. Thermal ellipsoid plots are drawn at 30% level. Carbon atoms drawn as ball and stick and hydrogens omitted for clarity.

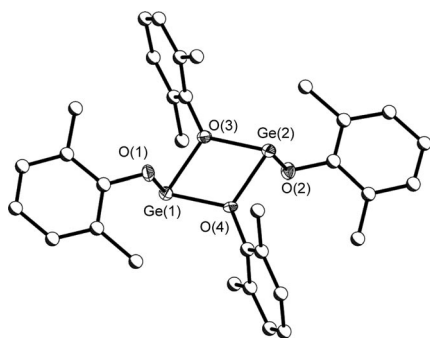


Figure 2. Structure plot of **2**. Thermal ellipsoid plots are drawn at 30% level. Carbon atoms drawn as ball and stick and hydrogens omitted for clarity.

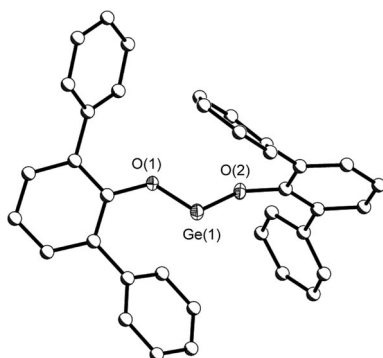


Figure 3. Structure plot of **3**. Thermal ellipsoid plots are drawn at 30% level. Carbon atoms drawn as ball and stick and hydrogens omitted for clarity.

oxides,^[66–71] the Ge–O terminal distances (av. 1.82 Å) are shorter than the Ge–(μ-O) bridging bond lengths (av. 1.98 Å). The internal Ge₂O₂ core has angles of (μ-O)–Ge–(μ-O) (av. 72.5°) and Ge–(μ-O)–Ge (av. 107.4°). These data are in agreement with the literature Ge(OR)₂ distances and angles^[45,84] Ge–O (av. 1.82 Å), Ge–(μ-O) (av. 1.98 Å), and (μ-O)–Ge–(μ-O) (av. 72.2°) Ge–(μ-O)–Ge (av. 107.5 Å). For the more sterically hindering DPP ligand, monomeric **3** was isolated in a bent arrangement as previously reported by

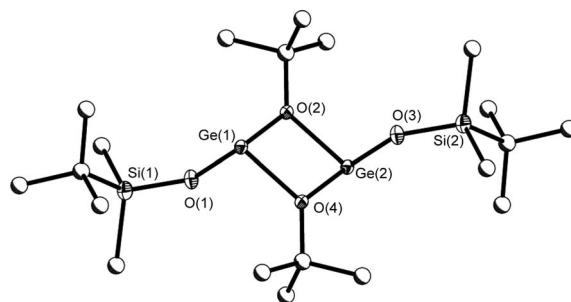


Figure 4. Structure plot of **4**. Thermal ellipsoid plots are drawn at 30% level. Carbon atoms drawn as ball and stick and hydrogens omitted for clarity.

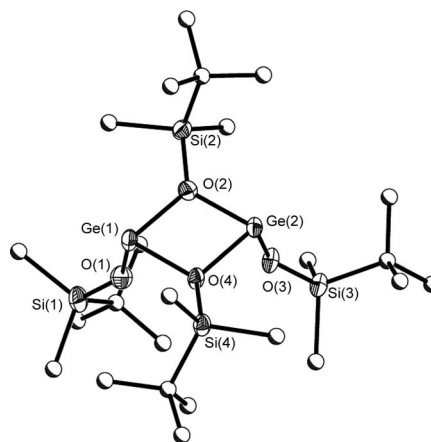


Figure 5. Structure plot of **5**. Thermal ellipsoid plots are drawn at 30% level. Carbon atoms drawn as ball and stick and hydrogens omitted for clarity.

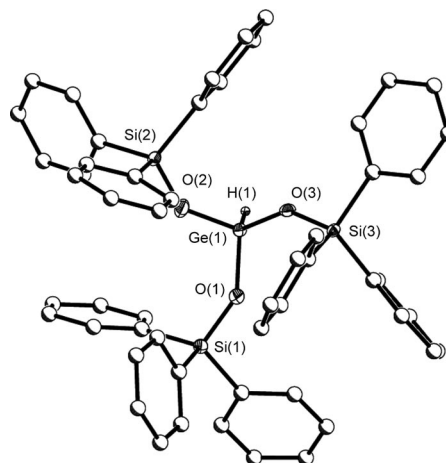


Figure 6. Structure plot of **6**. Thermal ellipsoid plots are drawn at 30% level. Carbon atoms drawn as ball and stick and hydrogens omitted for clarity.

Rothwell and co-workers;^[45] however, for this crystal solution, **3** was solved in the higher-ordered orthorhombic space group. The Ge–O bond length of 1.81 Å and O–Ge–O angle of 90.2° are in good agreement with previously reported Ge–O bond lengths of av. 1.82 Å and O–Ge–O angles of av. 91.6°.^[45]

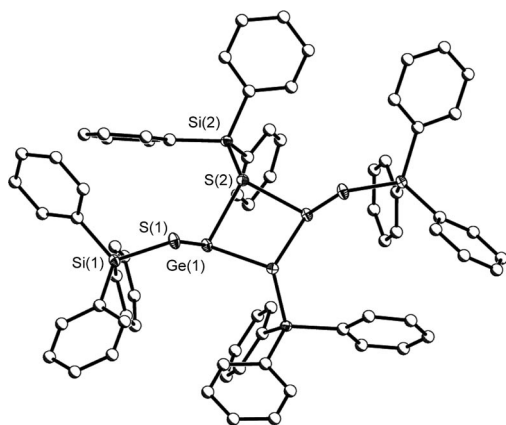


Figure 7. Structure plot of **7**. Thermal ellipsoid plots are drawn at 30% level. Carbon atoms drawn as ball and stick and hydrogens omitted for clarity.

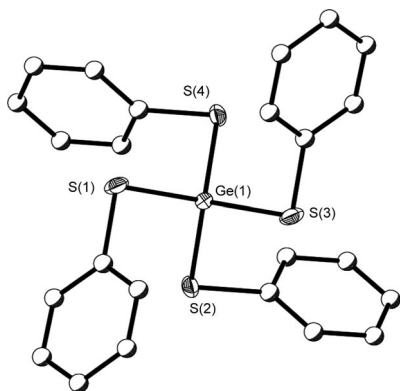


Figure 8. Structure plot of **8**. Thermal ellipsoid plots are drawn at 30% level. Carbon atoms drawn as ball and stick and hydrogens omitted for clarity.

It was of interest to determine what effect siloxide ligands would have on the final structure of Ge^{II} species. The first attempt to generate a homoleptic precursor following an alcoholysis exchange [Equation (2)] yielded the heteroleptic structure of **4** (Figure 4). For this compound only the terminal *OtBu* groups were substituted by DMBS ligands, leaving the original dinuclear pyramidal arrangement around the Ge metal centers intact. The two bridging *OtBu* groups had a $(\mu\text{-O})\text{-Ge}(\mu\text{-O})$ angle of av. 74.5° with $\text{Ge}(\mu\text{-O})$ distance of av. 1.96 \AA , and terminal Ge-O distance of av. 1.80 \AA , similar to the metrical data of $[\text{Ge}(\mu\text{-O}t\text{Bu})(\text{TPS})_2]_2$:^[47] $(\mu\text{-O})\text{-Ge}(\mu\text{-O})$ av. 74.8° ; Ge-O_{TPS} av. 1.81 \AA ; $\text{Ge}(\mu\text{-O}t\text{Bu})$ av. 1.96 \AA .

Attempts to generate homoleptic siloxides were realized following the transamination methodology [Equation (1)]. Using two equivalents of H-DMBS or H-TPS led to the fully substituted species **5** (Figure 5) and **6** (Figure 6), respectively. Interestingly, the DMBS derivative **5** adopted a dinuclear arrangement where the terminal DMBS ligands of the pyramidal Ge were found in a *cis* conformation. This unusual arrangement for Ge^{II} species forces a small out-of-plane twist (4.22°) of the Ge_2O_2 core. The terminal Ge-O

distances of $(\text{TPS})_2\text{Ge}\{[(\text{TMS})\text{N}=\text{P}(\text{Ph})_2]_2(\text{CH}_2)\}_2$,^[64] $(\text{porph})\text{Ge}(\text{TPS})_2$, and $[(\text{TPS})\text{Ge}(\mu\text{-O}t\text{Bu})_2]_2$ ^[47] av. 1.80 ,^[78] 1.86 ,^[64] and 1.81 ^[47] \AA , respectively are significantly longer in comparison to those noted for **5** (av. 1.78 \AA). This variation is most likely a reflection of the dinuclear, homoleptic nature of **5** in comparison to the other compounds. Further comparisons were made only to the dinuclear heteroleptic $[(\text{TPS})\text{Ge}(\mu\text{-O}t\text{Bu})_2]_2$.^[47] The internal core distances and angles of **5** [$\text{Ge}(\mu\text{-O})$ av. 1.98 \AA , with $\text{O-Ge}(\mu\text{-O})$ angles av. 96.0° and $(\mu\text{-O})\text{-Ge}(\mu\text{-O})$ av. 78.0°] appear to be roughly in agreement with $[(\text{TPS})\text{Ge}(\mu\text{-O}t\text{Bu})_2]_2$ ^[47] [$\text{Ge}(\mu\text{-O})$ av. 1.96 \AA , with $\text{O-Ge}(\mu\text{-O})$ angles av. 96.3° and $(\mu\text{-O})\text{-Ge}(\mu\text{-O})$ av. 74.7°]. In contrast to what was noted in the FTIR, there were no $\text{CH}_2\text{-H}\cdots\text{Ge}$ interactions observed in the solid-state structure of **5**.

For **6**, a monomer was isolated with three TPS groups, which suggests that either one of the TPS ligands is protonated or a hydride formed. The FTIR spectrum (vide infra) and ^1H NMR (vide supra) data indicated that the latter interpretation was the most appropriate. Further analysis of the electron density map of **6** revealed the presence of a proton located as part of the tetrahedral geometry around the Ge metal center (Figure 6). While the formation of the unusual compound **6** is not fully understood, a potential mechanism would include the initial formation of the homoleptic $\text{Ge}(\text{TPS})_2$ species, followed by additional coordination of free H-TPS, subsequent β -hydrogen transfer, and conversion to the Ge^{IV} hydride species **6**. This is consistent with previously disseminated mechanisms of Ge-H formation for other siloxide systems.^[45,80,85] The Ge-H bond length was resolved at 1.26 \AA , which is shorter than the recently published $[\text{Ge}(\text{H})(\mu\text{-O}_3\text{SiR})_4]$, $\text{R} = \text{N}(2,6\text{-}i\text{Pr}_2\text{C}_6\text{H}_3)\text{-}(\text{SiMe}_3)$, where the av. Ge-H bond length was 1.39 \AA .^[80] The short Ge-H bond length is attributed to the decreased electron donation capability of the attached TPS ligands; this is further evidenced in the Ge-H increased ^1H NMR shift downfield. The remainder of the metrical data (Ge-O av. 1.73 \AA , O-Ge-O angles av. 107.5° , H-Ge-O angles of av. 111.3°) are in agreement with $[\text{Ge}(\text{H})(\mu\text{-O}_3\text{SiR})_4]$ (Ge-O av. 1.74 \AA , for O-Ge-O av. 108.8° , H-Ge-O av. 109.9°).^[80]

Attempts to expand the ligand set to include thiolates were undertaken following Equation (1), which yielded **7** (see Figure 7). Compound **7** was found to be dinuclear with two bridging and two terminal *cis* TPST ligands, arranged in a pyramidal geometry around the Ge cations. While four $\text{Ge}^{\text{IV}}\text{-S-Si}$ species are available in the literature,^[86-89] **7** is the first report of a $\text{Ge}^{\text{II}}\text{-S-Si}$ complex, which complicates metrical comparisons. The TPST species has a Ge_2S_4 core that is significantly distorted from planarity (56.2°) with angles of av. 78.4° ($\mu\text{-S})\text{-Ge}(\mu\text{-S})$ and av. 93.0° ($\text{S})\text{-Ge}(\mu\text{-S})$ and distances of av. 2.32 \AA for Ge-S and av. 2.47 \AA $\text{Ge}(\mu\text{-S})$. These distances and angles do not compare favorably with the only appropriate model $[\text{Ge}(\mu\text{-S}t\text{Bu})(\text{S}t\text{Bu})_2]_2$:^[79] 27.6° twist of the Ge_2S_4 , angles of av. 85.5° ($\mu\text{-S})\text{-Ge}(\mu\text{-S})$, 92.1° ($\text{S})\text{-Ge}(\mu\text{-S})$, and distances of 2.43 \AA for Ge-S . The metrical variations must be due to changes in the steric bulk and electron donation of the SSiR_3 group of **7** to the SR group of $[\text{Ge}(\mu\text{-S}t\text{Bu})(\text{S}t\text{Bu})_2]_2$.^[79]

The use of the thiol H-PS in Equation (1) produced **8** (Figure 8), a monomeric species that has four PS ligands arranged in a distorted tetrahedral geometry around the Ge metal center. Since both the IR and ^1H NMR spectroscopic data indicate the removal of the protons from the PS ligands and the metrical aspects of **8** were comparable to the Ge^{IV} thiol species,^[65,90–93] **8** is considered to be in the +4 oxidation state instead of coordination of two H-PS ligands. In particular, the av. Ge–S distance of **8** was found to be 2.21 Å which favorably compares to the Ge^{IV} –S literature distances (av. 2.24 Å; range 2.19–2.412 Å)^[65,94] and not with Ge^{II} –S terminal distances (av. 2.32 Å; range 2.26–2.37 Å).^[65,79]

Elemental analyses of samples **1–8** revealed that the dried bulk crystalline materials are in agreement with the single crystal structures obtained for **1–8**. For **6**, it was necessary to subtract the lattice toluene molecule from the elemental composition to obtain an acceptable analysis.

Solution Behavior

Since these compounds are dissolved prior to nanocrystal processing, it is of interest to understand the solution behavior of these compounds. Therefore, crystalline materials of **1–8** were individually dissolved in either $[\text{D}_8]\text{tol}$ or CDCl_3 , flame-sealed in an NMR tube, and variable temperature ^1H NMR spectra (VT-NMR range –20 to +45 °C) obtained for each sample. No significant changes were noted in the NMR spectra over this temperature range for all of the samples, unless specifically discussed below.

For **1**, two sets of resonances were expected for the ethylene and methylene protons based on the asymmetry generated by the $\mu\text{-c-DBED}$ ligand. Upon dissolution in $[\text{D}_8]\text{tol}$, singlets at $\delta = 4.00$ and $\delta = 2.92$ tentatively assigned to the ethylene and methylene moieties, respectively were observed. This indicates a monomer exists in solution; however, the ^{13}C NMR spectroscopic data revealed two sets of resonances that substantiates that the solid-state structure of **1** is maintained in solution. The dinuclear **2** in $[\text{D}_8]\text{tol}$ also displayed a broad singlet for the 2,6-methyl groups of the aryloxide at $\delta = 2.25$ but in contrast to **1**, the ^{13}C spectrum revealed only one set of resonances, suggesting **2** favored a monomer in solution. However, VT-NMR studies on $[\text{Ge}(\mu\text{-DIP})(\text{DIP})_2]$ indicate that this compound main-

tains its nuclearity upon dissolution, with rapid exchange of the bridging and terminal ligands.^[45] Unfortunately, the lowered solubility of **2** favors precipitation at reduced temperatures, which prevents similar studies and therefore definite statements concerning its nuclearity in solution, cannot be made. In CDCl_3 , **3** revealed a complex multiplet ranging from $\delta = 7.56\text{--}7.04$ assigned to the numerous phenyl protons associated with the DPP ligand. Since it appears that a monomer may be structurally favored for **2** in solution, it would also follow that the more sterically demanding DPP ligand of **3** would also favor a monomeric species in solution.

The mixed alkoxide/siloxide species **4**, in CDCl_3 , presented an NMR spectra with singlets at $\delta = 1.41, 0.90,$ and 0.06 ppm, assigned to the $\text{OC}(\text{CH}_3)_3$, $\text{OSi}(\text{CH}_3)_2[\text{C}(\text{CH}_3)_3]$, and $\text{OSi}(\text{CH}_3)_2[\text{C}(\text{CH}_3)_3]$ moieties, respectively. Two complete set of ^{13}C NMR resonances and a single ^{29}Si NMR resonance at $\delta = 15.5$ ppm were found for **4**. Combined it is not possible to determine the nuclearity of **4**; however, since the previously reported $[\text{Ge}(\mu\text{-OtBu})(\text{TPS})_2]$ derivative^[47] was reported to be dinuclear in solution, it is reasonable to think **4** maintains the same central core in solution, with the sterically less demanding DMBS in place of the TPS. For compound **5** dissolved in CDCl_3 , the ^1H ($\delta = 1.81$ and 1.01 ppm), ^{13}C , and ^{29}Si peak ($\delta = 15.5$ ppm) revealed only one set of DMBS *t*Bu and methyl group resonances. This indicates that **5** is a monomer in solution.

Compound **6** displayed a sharp singlet at $\delta = 6.49$ ppm which is farther upfield in comparison to the reported ^1H shift of $[\text{Ge}(\text{H})(\mu\text{-O}_3\text{SiR})_4]$ at $\delta = 5.83$ ppm;^[80] however, this data combined with the other analytical data and crystal structure solution, leads to the assignment of **6** as the hydride. Examination of **7**, in CDCl_3 , lead to the identification of multiplets in the expected range of $\delta = 7.39\text{--}7.22$. Attempts to distinguish between mononuclear and dinuclear species was undertaken using VT NMR; however, the lack of dynamic behavior noted for **7** indicates that a single species is most likely present in solution. While the ^{13}C NMR spectroscopic data was complex and did not add any significant structural information, the ^{29}Si singlet at $\delta = -13.5$ ppm argues for the presence of a monomer in solution. Mononuclear **8** was found to have multiplets in the range of $\delta = 7.36\text{--}7.20$ with no indication of a hydride resonance. Table 1 lists the observed NMR solution behavior for these precursors.

Table 1. Structural^[a] and analytical data for **1–8**.

	Ligand type	Solid-state structure	Solution behavior	Dec. temp. [°C]	Nano morph.	AR	EDS	PXRD
1	NR ₂	di	di	180	ND	1	Ge	Ge ⁰ /cubic
2	OR	di	mono	200	NW	20	Ge	Ge ⁰ /cubic
3	OR	mono	mono	200–300	NW	13	Ge	Ge ⁰ /cubic
4	OR/OSiR ₃	di	di	130	– ^[b]	–	–	–
5	OSiR ₃	di	mono	110	NW	50	Ge	Ge ⁰ /cubic
6	OSiR ₃	mono (+4)	mono	200–280	NW	50	Ge	Ge ⁰ /cubic
7	SSiR ₃	di	mono	260–400	amorphous	NA	Ge/S	amorphous
8	SR	mono (+4)	mono	230	–	–	–	–

[a] AR = aspect ratio, ND = nanodot, NW = nanowire. [b] Not used as a precursor (–).

Thermal Gravimetric Analysis

In order to gain insight into the decomposition temperature differences for these precursors and their suitability for nanomaterials production, TGA data were collected for each compound, values given in parentheses are temp., % wt.-loss/calcd. % wt.-loss: **1** (180 °C, 76/ 76), **2** (200 °C, 82/77), **3** (200–300 °C, 87/87), **4** (130 °C, 85/74), **5** (110 °C, 88/78), **6** (200–280 °C, 60/61), **7** (260 °C, 81/89), and **8** (230 °C, 83/86). In general, the data for **1–8** (see Figure 9) indicated that the initiation of the organic decomposition occurred at temperatures that were acceptable for the preparatory routes of interest. It should also be noted that for **7**, a lower than expected weight loss was observed which may be explained by the cleavage of the Si–S linkage [i.e., loss of Si(C₆H₅), 79% weight loss], forming a Ge–S complex, which gradually loses sulfur as the temperature, exceeds 400 °C. The metrical listing of the decomposition temperature of these compounds is included in Table 1.

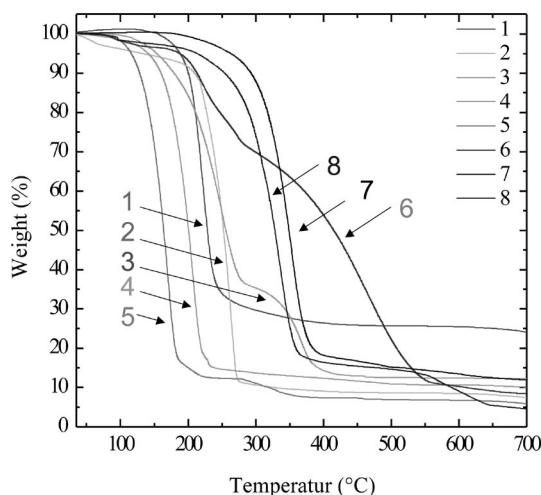


Figure 9. TGA of compounds **1–8**.

Nanomaterials

With a set of acceptable precursors that were amenable to our processing routes, the production of Ge⁰ nanomaterials was undertaken. The use of a simple solution route employing the non-coordinating octadecene as the main solvent was selected for the ease of interpretation of any possible PSA phenomenon. The Ge precursors **1–8** isolated for this study varied in both structural and electronic configuration, which made these a reasonable set of compounds to begin our study. Compound **4** was removed from consideration, since a heteroleptic ligand set would lead to confusion in what ultimately determined the final nanomaterial properties. Since both **6** and **8** were Ge^{IV} species, they were not investigated in the initial study. Compounds **1–3** and **5–7** were thought to be acceptable precursors and used for Ge⁰ nanomaterials production. For each reaction, dried crystalline powders of the respective precursors were used to minimize any contamination of the final nanomaterials generated.

The PXRD pattern of the products isolated from the reaction of **1–3**, and **5** were collected and found to be consistent with Ge⁰ with a preferred crystalline cubic structure (PDF # 04–0545), see Figure 10. Since the materials are nanopowders, the resulting patterns were broad and due to this fact, it is not possible to rule out the potential inclusion of amorphous Ge nanomaterials in the resulting powders.^[35,36] Transmission electron microscopy analyses were obtained on these materials and their images are shown in Figure 11 (a–e) for **1**, **2**, **3**, and **5**, respectively. The results obtained in this work are consistent with the previously disseminated efforts for production of Ge⁰.^[10,11,21] For **1**, the nanoparticles isolated appear to be 5 nm in diameter and agglomerated (Figure 11, a). In contrast compounds **2**, **3**, and **5** formed nanowires with a diameter (*d*) and aspect ratio (AR) for the compound given [*d* (nm)/AR]: **2** (14/20, Figure 11, b); **3** (7/13, Figure 11, c); **5** (5–17 up to 50, Figure 11, d). EDS analyses confirmed that Ge was formed in each sample. Additional powder XRD and EDS patterns concerning these compounds can be found in the Supporting Information.

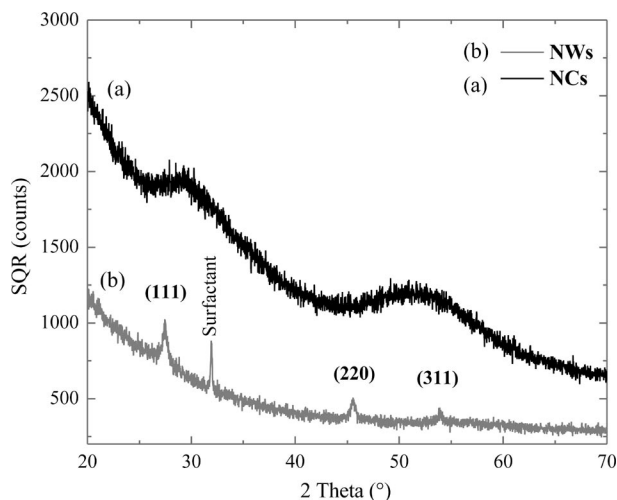


Figure 10. Powder XRD of Ge⁰ nanocrystals from **1** and nanowires from **5** showing the characteristic cubic germanium crystal structure.

With the successful production of Ge⁰ nanomaterials it was of interest to compare these results with the previous Ge^{II} precursors^[10,11,21] to elucidate any PSA influences. Under identical conditions, Ge[N(SiMe₃)₂]₂ was found to produce 5 nm Ge⁰ nanodots, whereas Ge(DBP)₂ (DBP = 2,6-dibutylphenol) formed Ge⁰ nanowires av. 20 nm in diameter (AR = 20).^[21] It is of note that Ge[N(SiMe₃)₂]₂ has been reported to form ca. 60 nm wires from a chemical vapor route when a Si₃C_xN_y shell is employed.^[19] Compound **1** allowed for a direct comparison to the previous amide results. High resolution TEM revealed that the resulting nanomaterials from **1** were a conglomerate of nanoparticles that were similar in shape and size of those generated by Ge[N(SiMe₃)₂]₂.^[21] Therefore, the diamine did not drastically alter the morphological properties of the resultant nanomaterials.^[59,60,75]

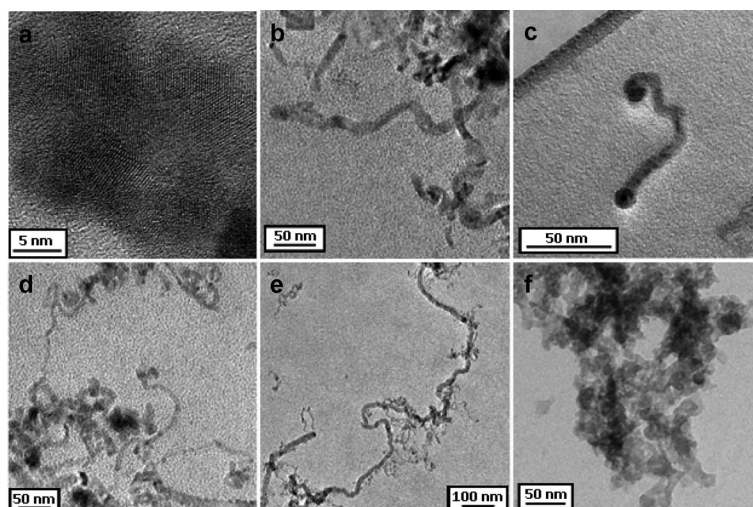


Figure 11. TEM images of Ge-based nanomaterials synthesized from: (a) **1**, (b) **2**, (c) **3**, (d) **5**, (e) **6**, (f) **7**.

For the alkoxy ligated compounds **2** and **3**, the decomposition results were also found to be in-line with the previous $\text{Ge}(\text{DBP})_2$ complex.^[21] The smaller wire diameters and lengths noted for **3** suggests that the sterically demanding DPP ligand slows the nucleation and growth of the wires as compared to the DMP ligand of **2** or the DBP ligand of $\text{Ge}(\text{DBP})_2$.^[21] This slower nucleation and growth could reasonably be attributed to the two-step decomposition pathway of the DPP ligands noted in the TGA (Figure 9).

For **5**, a significant difference in decomposition temperature was noted for the homoleptic siloxide precursors. For **5**, the Ge^{II} precursor's low decomposition temperature and lack of steric bulk would suggest that a dot morphology should prevail. However, significant amounts of nanowires were noted in the various TEM images which indicates that the lower thermal decomposition temperatures noted in the TGA (Figure 9) does *not* play a significant role in the final morphological properties of these compounds in this system. The nanowires' lengths were under a micron but were much longer than those formed from **2** and **3**. Again, the differing factor was the DMBS ligand, which suggests that siloxides favor longer growth times based on slower decomposition, forming nanowires.

Due to the success of high AR nanowires formed by the siloxide of **5**, coupled with the presence of the hydride, compound **6** became of interest to determine if this Ge^{IV} precursor could be converted in our system and how this effected the final morphologies observed. The Ge^{IV} siloxane precursor **6**, was expected to result in a wire-like material due to the similar decomposition temperature and bulky alkoxy ligands of $\text{Ge}(\text{DBP})_2$. The PXRD pattern indicated that Ge^0 had indeed been produced and TEM analyses revealed nanowires with widths that ranged from 5–25 nm with the larger diameter wires having an AR of up to 50 (Figure 11, e) had been formed. These AR are significantly longer than the nanowire lengths of **2** and **3**, and indicate that there may be a significant advantage using siloxide precursors for nanowire production.

The thiol derivative **7** was also processed to determine how these thiol precursors would behave in our system. Based on the TGA data, the silanethiolate **7** was expected to follow a similar decomposition route as the previous compounds and yield either a Ge^0 or a Ge–S nanomaterial. After processing, a broad PXRD pattern of the materials generated from **7** indicated that an amorphous material had been formed. TEM analysis revealed no distinguishable morphology (Figure 11, f) but EDS analysis indicated that both Ge and S were present in the nanomaterials; therefore, the material is thought to be an amorphous Ge_xS_y material. A higher processing temperature is obviously required to complete the decomposition/crystallization of **7**.^[95] These results also indicate that **7** was not suitable for Ge^0 nanomaterial syntheses.

Summary and Conclusions

This study increased the number of structurally characterized Ge^{II} precursors synthesized from either a transamination or alcoholysis metathesis reaction, including diamide (**1**), alkoxy (**2**, **3**), siloxide (**4**, **5**), silanethiolate (**7**), as well as Ge^{IV} hydride-siloxide (**6**), and thiolate (**8**) derivatives. Upon thermal decomposition of these compounds, it was found that nanodots were observed for **1**, while the majority (**2**, **3**, **5**, and **6**) of compounds formed nanowires (alkoxides: AR = 20; siloxides: AR = 50). The variation between the alkoxy and siloxide nanowire AR is of interest and further work to understand the factors behind this phenomenon are underway. The results from this study in general indicate the PSA plays a role in the resulting nanoparticle morphology;^[21] however, it is also obvious from these results that additional parameters and experimental approaches are required to garner the desired control to generate tailored Ge^0 nanomaterials. Studies are currently underway to determine how further system adjustments (i.e., temperature, reaction time, concentration, sterics, electronics, etc.)

influence the decomposition of the prescribed precursors and subsequent evolution of crystalline Ge-based nanomaterials.

Experimental Section

General: All compounds described below were handled with rigorous exclusion of air and water using standard Schlenk line and glove box techniques. All solvents were stored under argon and used as received (Aldrich) in SureSeal™ bottles, including hexanes (hex), toluene (tol), [D₈]toluene ([D₈]tol), [D₆]acetone, and [D]chloroform (CDCl₃). The following chemicals were used as received (Aldrich): GeCl₂·dioxane, LiN(SiMe₃)₂, H₂-DBED, H-OrBu, H-DMP, H-DPP, H-DMBS, H-TPS, H-TPST, H-PS, oleylamine, and octadecene. Ge[N(SiMe₃)₂]₂^[59,60,75] and [Ge(OrBu)₂]₂^[47,76] were synthesized according to literature reports.

General Synthesis: Due to the similarity of the following reactions a general preparation is presented with specific details presented for each reaction below. In a glovebox, the appropriate ligand was dissolved in a minimum amount of toluene and added via pipette to a stirring mixture of Ge(NR₂)₂ dissolved in toluene. After stirring for 10 min, the resulting reaction mixture was set aside and the volatile portion was allowed to slowly evaporate until light yellow or colorless X-ray quality crystals were isolated.

[Ge(μ_c-DBED)]₂ (1): Used H₂-DBED (0.198 g, 0.824 mmol), Ge(NR₂)₂ (0.324 g, 0.824 mmol), in tol (≈ 5 mL); yield 55.0% (0.258 g). FTIR (KBr pellet): $\tilde{\nu}$ = 3064 (s), 3025 (m), 2912 (m), 2885 (m), 2850 (w), 2821 (m), 2793 (m), 2770 (w), 1599 (s), 1491 (m), 1450 (w), 1356 (m), 1304 (m), 1211 (m), 1153 (w), 1065 (w), 1010 (m), 872 (w), 745 (w), 701 (w), 635 (w) cm⁻¹. ¹H NMR (250.0 MHz, [D₈]tol): δ = 7.13–7.23 [m, 10 H, (C₆H₅)CH₂N(CH)₂NCH₂(C₆H₅)], 4.00 [s, 2 H, (C₆H₅)CH₂N(CH)₂NCH₂(C₆H₅)], 2.92 [s, 4 H, (C₆H₅)CH₂N(CH)₂NCH₂(C₆H₅)] ppm. ¹³C NMR (62.86 MHz, CDCl₃): δ = 141.5, 129.0, 128.5, 128.4, 128.3, 127.1, 126.8 (C₆H₅)CH₂N(CH)₂NCH₂(C₆H₅), 54.4, 54.1, 52.4, 49.4, (C₆H₅)CH₂N(CH)₂NCH₂(C₆H₅) ppm. C₃₂H₃₆Ge₂N₄ (621.83): calcd. C 61.81, H 5.84, N 9.01; found C 62.14, H 5.72, N 9.16.

[Ge(μ-DMP)(DMP)]₂ (2): Used H-DMP (0.191 g, 1.56 mmol), Ge(NR₂)₂ (0.308 g, 0.782 mmol), in tol (≈ 5 mL); yield 90.8% (0.224 g). FTIR (KBr pellet): $\tilde{\nu}$ = 3038 (m), 3019 (m), 2978 (m), 2951 (m), 2914 (m), 2856 (m), 1590 (m), 1468 (w), 1262 (w), 1195 (w), 1168 (w), 1091 (w), 840 (w), 830 (w), 773 (w), 761 (w), 741 (w), 693 (w), 680 (w), 611 (m), 584 (w), 535 (m), 525 (m), 437 (w) cm⁻¹. ¹H NMR (250.0 MHz, [D₈]tol): δ = 7.00 [d, *J*_{H,H} = 3.75 Hz, 2 H, OC₆H₃(CH₃)₂], 6.73 [m, 1 H, OC₆H₃(CH₃)₂], 2.25 [s, 6 H, OC₆H₃(CH₃)₂] ppm. ¹³C NMR (62.86 MHz, CDCl₃): δ = 152.2, 129.8, 129.0, 123.7 [OC₆H₃(CH₃)₂], 17.4 [OC₆H₃(CH₃)₂] ppm. C₃₂H₃₆Ge₂O₄ (629.79): calcd. C 61.03, H 5.76; found C 60.57, H 5.96.

Ge(DPP)₂ (3): Used H-DPP (0.623 g, 2.53 mmol), Ge(NR₂)₂ (0.498 g, 1.27 mmol), in tol (≈ 5 mL); yield 80.6% (0.575 g). FTIR (KBr pellet): $\tilde{\nu}$ = 3080 (s), 3060 (m), 3051 (m), 3034 (s), 1595 (m), 1493 (m), 1455 (w), 1439 (m), 1408 (w), 1276 (m), 1241 (m), 1216 (w), 1085 (m), 1071 (m), 1028 (m), 842 (w), 761 (w) 746(w), 701 (w), 637 (w), 625 (m), 609 (w), 586 (m) cm⁻¹. ¹H NMR (250.0 MHz, CDCl₃): δ = 7.56 [d, *J*_{H,H} = 3.75 Hz, 4 H, OC₆H₃(C₆H₅)₂], 7.45 [m, 4 H, OC₆H₃(C₆H₅)₂], 7.36 [m, 2 H, OC₆H₃(C₆H₅)₂], 7.28 [d, *J*_{H,H} = 3.75 Hz, 2 H, OC₆H₃(C₆H₅)₂], and 7.04 [m, 1 H, OC₆H₃(C₆H₅)₂] ppm. C₃₆H₂₆GeO₂ (563.16): calcd. C 76.78, H 4.65; found C 77.36, H 4.92.

[Ge(μ-OrBu)(DMBS)]₂ (4): Used [Ge(OrBu)₂]₂^[47,76] (0.440 g, 1.00 mmol), H-DMBS (0.266 g, 2.01 mmol), in hexanes (≈ 5 mL); yield 86.2% (0.480 g). FTIR (KBr pellet): $\tilde{\nu}$ = 2958 (w), 2931 (w), 2894 (m), 2857 (m), 1467 (m), 1388 (m), 1365 (m), 1251 (w), 1177 (m), 952 (w), 891 (w), 833 (w), 775 (w), 727 (m), 673 (s), 603 (w) cm⁻¹. ¹H NMR (250.0 MHz, CDCl₃): δ = 1.41 [s, 9 H, OC(CH₃)₃], 0.90 [s, 9 H, OSi(CH₃)₂C(CH₃)₃], 0.06 [s, 6 H, OSi(CH₃)₂C(CH₃)₃] ppm. C₂₀H₄₈Ge₂O₄Si₂ (553.94): calcd. C 43.36, H 8.73; found C 43.08, H 8.71.

[Ge(μ-DMBS)(DMBS)]₂ (5): Crystals were obtained by reduction of solvent and subsequent refrigeration (–30 °C) over 24 h. Used H-DMBS (0.232 g, 1.75 mmol), Ge(NR₂)₂ (0.345 g, 0.877 mmol), in tol (≈ 5 mL); yield 97.0% (0.285 g). FTIR (KBr pellet): $\tilde{\nu}$ = 2954 (w), 2933 (w), 2890 (w), 2859 (w), 2131 (m), 1468 (m), 1408 (s), 1391 (s), 1361 (s), 1255 (w), 956 (w), 836 (w), 805 (w), 779 (w), 725 (w), 679 (m), 593 (m), 541 (s) cm⁻¹. ¹H NMR (250.0 MHz, CDCl₃): δ = 1.81 [s, 9 H, OSi(CH₃)₂C(CH₃)₃], 1.01 [s, 6 H, OSi(CH₃)₂C(CH₃)₃] ppm. ²⁹Si NMR (49.66 MHz, [D₈]tol): δ = 15.5 [OSi(CH₃)₂C(CH₃)₃] ppm. ¹³C NMR (62.86 MHz, [D₈]tol): δ = 25.9 [OSi(CH₃)₂C(CH₃)₃], 18.5 [OSi(CH₃)₂C(CH₃)₃], –2.50 [OSi(CH₃)₂C(CH₃)₃] ppm. C₂₄H₆₀Ge₂O₄Si₄ (670.26): calcd. C 43.01, H 9.02; found C 42.81, H 8.64.

Ge(TPS)₃(H) (6): Used H-TPS (1.98 g, 7.16 mmol), Ge(NR₂)₂ (0.939 g, 2.39 mmol), in tol (≈ 20 mL); yield 93.1% (2.00 g). FTIR (KBr): $\tilde{\nu}$ = 3067 (m), 3050 (m), 3022 (w), 3012 (w), 2998 (w), 2130 (m), 1588 (w), 1425 (s), 1115 (s), 971 (s), 721 (s), 696 (s), 591 (m), 510 (s) cm⁻¹. ¹H NMR (250.0 MHz, CDCl₃): δ = 7.37 [d, *J*_{H,H} = 3.75 Hz, 2 H, OSi(C₆H₅)₃], 7.13 [m, 2 H, OSi(C₆H₅)₃], 6.49 (s, 1 H, H-Ge) ppm. C₅₄H₄₆GeO₃Si₃ (899.79): calcd. C 72.08, H 5.15; found C 72.18, H 5.51.

[Ge(μ-TPST)(TPST)]₂ (7): Colorless crystals were obtained by reduction of solvent and subsequent refrigeration (–30 °C) over 24 h. Used H-TPST (0.931 g, 1.59 mmol), Ge(NR₂)₂ (0.313 g, 0.796 mmol), in tol (≈ 5 mL); yield 75.2% (0.392 g). FTIR (KBr pellet): $\tilde{\nu}$ = 3357 (w), 3072 (m), 3048 (m), 3024 (w), 3013 (w), 2998 (w), 2958 (m), 2896 (w), 2855 (w), 1429 (s), 1116 (s), 736 (m), 702 (s), 534 (s), 514 (s), 503 (s), 486 (m) cm⁻¹. ¹H NMR (250.0 MHz, CDCl₃): δ = 7.39 [d, *J*_{H,H} = 3.75 Hz, 6 H, SSi(C₆H₅)₃], 7.31 [m, 6 H, SSi(C₆H₅)₃], 7.22 [m, 3 H, SSi(C₆H₅)₃] ppm. ²⁹Si NMR (49.66 MHz, CDCl₃): δ = –13.50 [SSi(C₆H₅)₃] ppm. C₇₂H₆₀Ge₂S₄Si₄ (1310.98): calcd. C 65.96, H 4.61; found C 65.33, H 4.57.

Ge(PS)₄ (8): After mixing, the solution produced a deep red oil with a light red solution. The light red solution was decanted off and allowed to dry in the glovebox atmosphere to produce X-ray quality crystals. Used H-PS (0.445 g, 5.12 mmol), Ge(NR₂)₂ (0.503 g, 1.28 mmol), in tol (≈ 10 mL); yield 62.3% (0.407 g). FTIR (KBr): $\tilde{\nu}$ = 3072 (w), 3053 (w), 2961 (m), 2924 (m), 2853 (w), 1577 (m), 1474 (m), 1466 (m), 1437 (m), 1095 (s), 1079 (s), 1022 (s), 737 (s), 688 (s) cm⁻¹. ¹H NMR (250.0 MHz, CDCl₃): δ = 7.36–7.20 (m, 5 H, SC₆H₅) ppm. C₂₄H₂₀GeS₄ (509.23): calcd. C 56.61, H 3.96; found C 56.69, H 3.64.

Precursor Characterization: Fourier Transform Infrared (FTIR) spectroscopic data were obtained on a Bruker Vector 22 Instrument using KBr pressed pellets with bulk material, under an atmosphere of flowing nitrogen. Elemental analyses were performed on a Perkin–Elmer 2400 CHN-S/O Elemental Analyzer. Reported nuclear magnetic resonance (NMR) spectroscopic data were collected on a 250 MHz Bruker instrument using crystalline material dissolved in [D₈]tol or CDCl₃. The ¹H and ¹³C NMR spectroscopic data were referenced against the residual protonated solvent, and 5% TMS in [D₆]acetone for ²⁹Si NMR spectroscopy. Thermogravimetric

analyses (TGA) were collected by a TA Instruments SDT Q600 on crystalline materials from room temperature to 700 °C at a 10 °C/min heating rate, under a flowing atmosphere of nitrogen.

General Single Crystal X-ray Structure Information: Crystals were mounted onto a glass fiber from a pool of Fluorolube™ and immediately placed in a cold N₂ vapor stream, on a Bruker AXS diffractometer equipped with a SMART 1000 CCD detector using graphite monochromatized Mo-K_α radiation ($\lambda = 0.7107 \text{ \AA}$). Lattice determination and data collection were carried out using SMART Version 5.054 software. Data reduction was performed using SAINTPLUS Version 6.01 software and corrected for absorption using the SADABS program within the SAINT software package.

Structures were solved by direct methods that yielded the heavy atoms, along with a number of the lighter atoms or by using the PATERSON method, which yielded the heavy atoms. Subsequent Fourier syntheses yielded the remaining light-atom positions. The hydrogen atoms were fixed in positions of ideal geometry and refined using SHELXS software. The final refinement of each compound included anisotropic thermal parameters for all non-hydrogen atoms. All final CIF files were checked at <http://www.iucr.org/>. Data collection parameters for 1–8 are given in Table 2. It is of note that crystal structures of M(OR)_x often contain disorder within the atoms of the pendant hydrocarbon chain, causing higher final correlations than is typically observed for other metalorganic structure solutions.^[66–71] The structures of 2 and 8 were solved with well-behaved thermal ellipsoids in the non-centrosymmetric orthorhombic space groups *Pca*₂₁ and *Pba*₂, respectively. For 2, the arrangement of DMP ligands in a *trans* fashion prohibits a mirror plane from bisecting the bridging DMP ligands in the orthorhom-

bic space group. In the case of 8, it should be noted that the selenium analog Ge(SePh)₄, where Ph = C₆H₅, also shares the same non-centrosymmetric orthorhombic space group *Pba*₂.^[96] For compound 6, a toluene molecule was located in the crystal lattice but due to significant disordering it was squeezed out to improve refinement values using the Platon (v. 1.11, 2007) program.

CCDC-705319 to -705326 contain the supplementary crystallographic data for 1–8, respectively. These data can be obtained free of charge from The Cambridge Crystallographic Data Centre via www.ccdc.cam.ac.uk/data_request/cif.

Nanoparticle Synthesis: The dried crystalline precursor (1.00 mmol) was dissolved in oleylamine and then rapidly injected into a solution of octadecene (10.0 mmol) preheated to 315 °C. The reaction temperature was maintained at 315 °C for 30 min and allowed to cool to room temperature. An aliquot of the Ge nanomaterial solution was dissolved in CHCl₃ and precipitated using MeOH, which was collected by centrifugation. After washing in this manner a minimum of three times, the collected Ge nanomaterials were dispersed in CHCl₃ and a drop was placed onto a TEM grid for subsequent analyses. It should be noted that size-selective precipitation methods were not utilized for TEM analyses.

Nanoparticle Characterization: Powder X-ray diffraction (XRD) was performed by a PANalytical X'Pert Pro XRD in the 2 θ range of 15–75° at a scan rate of 0.06°/s on drop-deposited Ge nanomaterials using a zero background holder. Transmission electron microscopy (TEM) analyses were performed on a JEOL JEM-2010 electron microscope equipped with an Oxford Instruments Energy Dispersive X-ray Spectroscopic (EDS) detector.

Supporting Information (see also the footnote on the first page of this article): Powder XRD patterns for 2, 3, 4, and 6.

Table 2. Crystal structure determination data collection parameters for 1–8.

Compound	1	2	3	4
Empirical formula	C ₃₂ H ₃₆ Ge ₂ N ₄	C ₃₂ H ₃₆ Ge ₂ O ₄	C ₃₆ H ₂₆ GeO ₂	C ₂₀ H ₄₈ Ge ₂ O ₄ Si ₂
Formula weight	621.83	629.79	563.16	553.94
Temperature [K]	144(2)	203(2)	203(2)	173(2)
Space group	monoclinic, <i>P</i> ₂ ₁ / <i>n</i>	orthorhombic, <i>Pca</i> ₂₁	orthorhombic, <i>Pccn</i>	monoclinic, <i>C</i> ₂ / <i>c</i>
<i>a</i> [Å]	8.7362(8)	17.014(5)	22.0568(19)	23.361(3)
<i>b</i> [Å]	9.1574(8)	10.879(3)	11.0189(9)	14.455(2)
<i>c</i> [Å]	18.7120(16)	16.282(5)	11.6412(10)	16.994(2)
β [°]	95.9070(10)			90.344(2)
<i>V</i> [Å ³]	1489.0(2)	3013.7(15)	2829.3(4)	5738.5(14)
<i>Z</i>	2	4	4	8
<i>D</i> _{calcd.} [mg/m ³]	1.386	1.388	1.324	1.282
μ (Mo-K _α) [mm ⁻¹]	2.045	2.028	1.115	2.198
<i>R</i> ₁ ^[a] (%) (all data)	6.02 (6.32)	6.15 (7.74)	2.85 (3.36)	3.41 (4.97)
<i>wR</i> ₂ ^[b] (%) (all data)	11.47 (11.59)	11.78 (12.37)	7.41 (7.74)	8.25 (9.18)
Compound	5	6	7	8
Empirical formula	C ₂₄ H ₆₀ Ge ₂ O ₄ Si ₄	C ₅₄ H ₄₆ GeO ₃ Si ₃	C ₇₂ H ₆₀ Ge ₂ S ₄ Si ₄	C ₂₄ H ₂₀ GeS ₄
Formula weight	670.26	899.79	1310.98	509.23
Temperature [K]	203(2)	203(2)	203(2)	203(2)
Space group	monoclinic, <i>P</i> ₂ ₁ / <i>c</i>	monoclinic, <i>P</i> ₂ ₁ / <i>n</i>	monoclinic, <i>C</i> ₂ / <i>c</i>	orthorhombic, <i>Pba</i> ₂
<i>a</i> [Å]	10.948(4)	21.580(3)	31.370(3)	8.595(5)
<i>b</i> [Å]	14.225(5)	9.9527(11)	9.2183(9)	16.852(10)
<i>c</i> [Å]	23.645(8)	24.529(3)	23.357(2)	8.142(5)
β [°]	90.336(5)	113.988(2)	105.996(2)	
<i>V</i> [Å ³]	3682.0(2)	4813.4(9)	6492.7(11)	1179.3(12)
<i>Z</i>	4	4	4	2
<i>D</i> _{calcd.} [mg/m ³]	1.209	1.242	1.341	1.434
μ (Mo-K _α) [mm ⁻¹]	1.786	0.753	1.170	1.661
<i>R</i> ₁ ^[a] (%) (all data)	7.71 (11.91)	4.80 (7.02)	5.59 (6.80)	4.69 (6.35)
<i>wR</i> ₂ ^[b] (%) (all data)	19.49 (21.60)	10.69 (11.54)	11.27 (11.77)	7.10 (7.65)

[a] $R_1 = \sum ||F_o| - |F_c|| / \sum |F_o| \times 100$. [b] $wR_2 = [\sum w(F_o^2 - F_c^2)^2 / \sum (w|F_o|^2)^2]^{1/2} \times 100$.

Acknowledgments

This work was partially funded by the National Science Foundation (NSF) under Grant NSF CBET-0756776, the Office of Basic Energy Sciences of the Department of Energy, and the National Institutes of Health (NIH) through the NIH Roadmap for Medical Research Grant #1 R21 EB005365-01. Information on this RFA (Innovation in Molecular Imaging Probes) can be found at <http://grants.nih.gov/grants/guide/rfa-files/RFA-RM-04-021.html>. Sandia is a multiprogram laboratory operated by Sandia Corporation, a Lockheed Martin Company, for the United States Department of Energy under contract DE-AC04-94AL85000.

- [1] X. An, R. Huang, X. Zhang, Y. Wang, *Semicond. Sci. Technol.* **2005**, *20*, 1034–1038.
- [2] A. Khakifirooz, D. A. Antoniadis, *Electron Device Lett.* **2004**, *25*, 80–82.
- [3] L. J. Lauhon, M. S. Gudiksen, C. L. Wang, C. M. Lieber, *Nature* **2002**, *420*, 57–61.
- [4] C. H. Tu, T. C. Chang, P. T. Liu, C. F. Weng, H. C. Liu, L. T. Chang, S. K. Lee, W. R. Chen, S. M. Sze, C. Y. Chang, *J. Electrochem. Soc.* **2007**, *154*, H435–H439.
- [5] K. Gacem, A. El Hdiy, M. Troyon, I. Berbezier, P. D. Szkutnik, A. Karmous, A. Ronda, *J. Appl. Phys.* **2007**, *102*, 093704–093707.
- [6] M. Kanoun, C. Busseret, A. Poncet, A. Souifi, T. Baron, E. Gautier, *Solid State Electron.* **2006**, *50*, 1310–1314.
- [7] A. D. Pasquier, D. D. T. Mastrogiovanni, L. A. Klein, T. Wang, E. Garfunkel, *Appl. Phys. Lett.* **2007**, *91*, 183501–183503.
- [8] R. Wang, Z. L. Guo, G. P. Wang, *Sol. Energy Mater. Sol. Cells* **2006**, *90*, 1052–1057.
- [9] M. P. Deshmukh, J. Nagaraju, *Sol. Energy Mater. Sol. Cells* **2005**, *89*, 403–408.
- [10] H. Gerung, T. J. Boyle, Y. Zhao, L. Wang, R. K. Jain, S. M. Han, *Appl. Phys. Lett.* **2006**, *89*, 111107–111109.
- [11] T. N. Lambert, N. L. Andrews, H. Gerung, T. J. Boyle, J. M. Oliver, B. S. Wilson, S. M. Han, *Small* **2007**, *3*, 691–699.
- [12] B. A. Hernandez-Sanchez, T. J. Boyle, T. N. Lambert, S. D. Daniel-Taylor, J. M. Oliver, B. S. Wilson, D. S. Lidke, N. L. Andrews, *IEEE Trans. Nanobiosci.* **2006**, *5*, 222–230.
- [13] S. M. Sze, in: *Physics of Semiconductor Devices*, 2nd ed., John Wiley & Sons, New York, **2002**.
- [14] R. Rosetti, R. Hull, J. M. Gibson, L. E. Brus, *J. Chem. Phys.* **1985**, *83*, 1406–1410.
- [15] T. Takagahara, K. Takeda, *Phys. Rev. B* **1992**, *46*, 15578–15581.
- [16] D. V. Melnikov, J. R. Chelikowsky, *Solid State Commun.* **2003**, *127*, 361–365.
- [17] C. Bostedt, T. van Buuren, T. M. Willey, N. Franco, L. J. Terminello, C. Heske, T. Moller, *Appl. Phys. Lett.* **2004**, *84*, 4056–4058.
- [18] J. H. Warner, R. D. Tilley, *Nanotechnology* **2006**, *17*, 3745–3749.
- [19] S. Mathur, H. Shen, N. Donia, T. Rugamer, V. Sivakov, U. Werner, *J. Am. Chem. Soc.* **2007**, *129*, 9746–9752.
- [20] D. Gerion, N. Zaitseva, C. Saw, M. F. Casula, S. Fakra, T. Van Buuren, G. Galli, *Nano Lett.* **2004**, *4*, 597–602.
- [21] H. Gerung, T. J. Boyle, L. J. Tribby, S. D. Bunge, C. J. Brinker, S. M. Han, *J. Am. Chem. Soc.* **2006**, *128*, 5244–5250.
- [22] Y. Y. Wu, P. D. Yang, *Chem. Mater.* **2000**, *12*, 605.
- [23] S. Mathur, H. Shen, V. Sivakov, U. Werner, *Chem. Mater.* **2004**, *16*, 2449.
- [24] A. M. Morales, C. M. Lieber, *Science* **1998**, *279*, 208–211.
- [25] T. Hanrath, B. A. Korgel, *J. Am. Chem. Soc.* **2002**, *124*, 1424–1429.
- [26] T. Hanrath, B. A. Korgel, *Adv. Mater.* **2003**, *15*, 437–440.
- [27] P. S. Shah, T. Hanrath, K. P. Johnston, B. A. Korgel, *J. Phys. Chem. B* **2004**, *108*, 9574–9587.
- [28] T. Hanrath, B. A. Korgel, *J. Am. Chem. Soc.* **2004**, *126*, 15466–15472.
- [29] R. S. Wagner, W. C. Ellis, *Appl. Phys. Lett.* **1964**, *4*, 89–90.
- [30] N. Zaitseva, J. Harper, D. Gerion, C. Saw, *Appl. Phys. Lett.* **2005**, *86*, 053105.
- [31] D. W. Wang, H. J. Dai, *Angew. Chem. Int. Ed.* **2002**, *41*, 4783–4786.
- [32] H. Gerung, S. D. Bunge, T. J. Boyle, C. J. Brinker, S. M. Han, *Chem. Commun.* **2005**, 1914–1916.
- [33] Y. N. Xia, P. D. Yang, Y. G. Sun, Y. Y. Wu, B. Mayers, B. Gates, Y. D. Yin, F. Kim, Y. Q. Yan, *Adv. Mater.* **2003**, *15*, 353–389.
- [34] J. Heath, F. Legoues, *Chem. Phys. Lett.* **1993**, *208*, 263–268.
- [35] B. R. Taylor, S. M. Kauzlarich, H. W. H. Lee, G. R. Delgado, *Chem. Mater.* **1998**, *10*, 22–24.
- [36] M. Xuchu, W. Fengyi, S. M. Kauzlarich, *J. Solid State Chem.* **2008**, *181*, 1628–1633.
- [37] A. J. Bard, R. Parsons, J. Jordan, in: *Standard Potentials in Aqueous Solutions*, IUPAC, New York, **1985**.
- [38] T. J. Boyle, B. A. Hernandez-Sanchez, C. M. Baros, M. A. Rodriguez, L. N. Brewer, *Chem. Mater.* **2007**, *19*, 2016–2026.
- [39] T. J. Boyle, S. D. Bunge, T. M. Alam, G. P. Holland, T. J. Headley, G. Avilucea, *Inorg. Chem.* **2005**, *44*, 1309–1318.
- [40] T. J. Boyle, S. D. Bunge, N. L. Andrews, L. E. Matzen, K. Sieg, M. A. Rodriguez, T. J. Headley, *Chem. Mater.* **2004**, *16*, 3279–3288.
- [41] C. Stanciu, M. Stender, A. F. Richards, M. M. Olmstead, P. P. Power, *Inorg. Chem.* **2005**, *44*, 2774–2780.
- [42] F. H. Allen, *Acta Crystallogr., Sect. B* **2002**, *58*, 380–388.
- [43] C. Stanciu, A. F. Richards, M. Stender, M. M. Olmstead, P. P. Power, *Polyhedron* **2006**, *25*, 477–483.
- [44] L. W. Pineda, V. Jancik, K. Starke, R. B. Oswald, H. W. Roesky, *Angew. Chem. Int. Ed.* **2006**, *45*, 2602–2605.
- [45] C. S. Weinert, A. E. Fenwick, P. E. Fanwick, I. P. Rothwell, *Dalton Trans.* **2003**, 532–539.
- [46] P. Bazinet, G. P. A. Yap, D. S. Richeson, *J. Am. Chem. Soc.* **2001**, *123*, 11162–11167.
- [47] M. Veith, C. Mathur, V. Huch, *J. Chem. Soc., Dalton Trans.* **1997**, 995–999.
- [48] A. Meller, G. Ossig, W. Maringgele, M. Noltemeyer, D. Stalke, R. Herbst-Irmer, S. Freitag, G. M. Sheldrick, *Z. Naturforsch. B: Chem. Sci.* **1992**, *47*.
- [49] T. Fjeldberg, P. B. Hitchcock, M. F. Lappert, S. J. Smith, A. J. Thorne, *J. Chem. Soc., Chem. Commun.* **1985**, 939–941.
- [50] M. F. Lappert, M. J. Slade, J. L. Atwood, M. J. Zaworotko, *J. Chem. Soc., Chem. Commun.* **1980**, 621–622.
- [51] B. Cetinkaya, I. Gumrukcu, M. F. Lappert, J. L. Atwood, R. D. Rogers, M. J. Zaworotko, *J. Am. Chem. Soc.* **1980**, *102*, 2088–2089.
- [52] F. E. Hahn, A. V. Zabula, T. Pape, A. Hepp, *Eur. J. Inorg. Chem.* **2007**, 2405–2408.
- [53] M. Driess, S. Yao, M. Brym, C. van Wullen, *Angew. Chem. Int. Ed.* **2006**, *45*, 4349–4352.
- [54] W. A. Herrmann, M. Denk, J. Behm, W. Scherer, F.-R. Klingan, H. Bock, B. Solouki, M. Wagner, *Angew. Chem. Int. Ed. Engl.* **1992**, *31*, 1485–1488.
- [55] I. L. Fedushkin, A. A. Skatova, V. A. Chudakova, N. M. Khvoynova, A. Y. Baurin, S. Dechert, M. Hummert, H. Schumann, *Organometallics* **2004**, *23*, 3714–3718.
- [56] O. Kuhl, P. Lonneck, J. Heinicke, *Polyhedron* **2001**, *20*, 2215–2222.
- [57] T. Gans-Eichler, D. Gudat, K. Nattinen, M. Nieger, *Chem. Eur. J.* **2006**, *12*, 1162–1173.
- [58] A. V. Zabula, F. E. Hahn, T. Pape, A. Hepp, *Organometallics* **2007**, *26*, 1972–1980.
- [59] A. Schnepf, *Z. Anorg. Allg. Chem.* **2006**, *632*, 935–938.
- [60] R. W. Chorley, P. B. Hitchcock, M. F. Lappert, W.-P. Leung, P. P. Power, M. M. Olmstead, *Inorg. Chim. Acta* **1992**, *198*, 203.
- [61] M. Veith, A. Rammo, *Z. Anorg. Allg. Chem.* **2001**, *627*, 662–668.
- [62] Y. Q. Ding, Q. J. Ma, H. W. Roesky, R. Herbst-Irmer, I. Uson, M. Noltemeyer, H. G. Schmidt, *Organometallics* **2002**, *21*, 5216–5220.

- [63] N. N. Zemlyansky, I. V. Borisova, M. G. Kuznetsova, *Organometallics* **2003**, *22*, 1675–1681.
- [64] W.-P. Leung, K.-W. Kan, C.-W. So, T. C. Mak, *Appl. Organomet. Chem.* **2007**, *21*, 814–818.
- [65] B. Kersting, B. Krebs, *Inorg. Chem.* **1994**, *33*, 3886–3892.
- [66] D. C. Bradley, *Chem. Rev.* **1989**, *89*, 1317–1322.
- [67] D. C. Bradley, R. C. Mehrotra, D. P. Gaur, *Metal Alkoxides*, Academic Press, New York, **1978**.
- [68] K. G. Caulton, L. G. Hubert-Pfalzgraf, *Chem. Rev.* **1990**, *90*, 969–995.
- [69] C. D. Chandler, C. Roger, M. J. Hampden-Smith, *Chem. Rev.* **1993**, *93*, 1205–1241.
- [70] L. G. Hubert-Pfalzgraf, *New J. Chem.* **1987**, *11*, 663–675.
- [71] N. Y. Turova, E. P. Turevskaya, V. G. Kessler, M. I. Yanovskaya, *The Chemistry of Metal Alkoxides*, Kluwer Academic Publishers, Boston, **2002**.
- [72] T. J. Boyle, L. J. Tribby, S. D. Bunge, *Eur. J. Inorg. Chem.* **2006**, 4553–4563.
- [73] M. F. P. Lappert, P. P. Sanger, A. R. Srivastava, R. C. in: *Metal and Metalloid Amides*, Halsted Press, Chichester, U. K., **1980**.
- [74] P. A. G. O'Hare, L. A. Curtiss, *J. Chem. Thermodynamics* **1995**, *27*, 643–662.
- [75] P. J. Davidson, D. H. Harris, M. F. Lappert, *J. Chem. Soc., Dalton Trans.* **1976**, 2268–2274.
- [76] M. Veith, J. Hans, L. Stahl, P. May, V. Huch, A. Sebald, *Z. Naturforsch., Teil B* **1991**, *16*, 403–424.
- [77] G. D. Smith, P. E. Fanwick, I. P. Rothwell, *Inorg. Chem.* **1990**, *29*, 3221–3226.
- [78] A. Krivokapic, H. L. Anderson, G. Bourhill, R. Ives, S. Clark, K. J. McEwan, *Adv. Mater.* **2001**, *13*, 652–656.
- [79] M. Veith, P. Hobein, R. Rosler, *Z. Naturforsch. B: Chem. Sci.* **1989**, *44*, 1067–1081.
- [80] U. N. Nehete, V. Chandrasekhar, H. W. Roesky, J. Magull, *Angew. Chem. Int. Ed.* **2005**, *44*, 281–284.
- [81] S. Patai, Z. Rappoport, in: *The Chemistry of Organic Germanium, Tin and Lead Compounds*, vol. 1–2, John Wiley & Sons, New York, **1995–2002**.
- [82] M. F. Lappert, J. L. Atwood, M. J. Zaworotko, A. J. Carty, *J. Organomet. Chem.* **1981**, *212*, C4–C6.
- [83] M. Lesbre, P. Mazerolles, J. Satgé in *The Organic Compounds of Germanium*, Wiley-Interscience, New York, **1971**, p. 702.
- [84] A. E. Weatherby Jr., L. R. Goeller, A. G. DiPasquale, A. L. Rheingold, C. S. Weinert, *Inorg. Chem.* **2007**, *46*, 7579–7586.
- [85] C. S. Weinert, *Main Group Met. Chem.* **2007**, *30*, 93–100.
- [86] G. Ossig, A. Meller, C. Bronneke, O. Muller, M. Schafer, R. Herbst-Irmer, *Organometallics* **1997**, *16*, 2116–2120.
- [87] U. Herzog, U. Bohme, E. Brendler, G. Rheinwald, *J. Organomet. Chem.* **2001**, *630*, 139–148.
- [88] U. Herzog, G. Rheinwald, *Organometallics* **2001**, *20*, 5369–5374.
- [89] U. Herzog, H. Borrmann, *J. Organomet. Chem.* **2003**, *675*, 42–47.
- [90] H. A. Klasens, H. J. Backer, *Recueil Trav. Chim. Pays-Bas* **1939**, *58*, 941–947.
- [91] J. Pfeiffer, M. Noltemeyer, A. Meller, *Z. Anorg. Allg. Chem.* **1989**, *572*, 145–150.
- [92] D.-H. Chen, H.-C. Chiang, C.-H. Ueng, *Inorg. Chim. Acta* **1993**, *208*, 99–101.
- [93] R. R. Holmes, R. O. Day, A. C. Sau, J. M. Holmes, *Inorg. Chem.* **1986**, *25*, 600–606.
- [94] J. E. Drake, A. G. Mislanker, J. Yang, *Inorg. Chem.* **1992**, *31*, 5543–5548.
- [95] A. Perakis, I. P. Kotsalas, E. A. Pavlatou, C. Raptis, *Phys. Stat. Sol. B* **1999**, *211*, 421–427.
- [96] H. J. Gysling, H. R. Luss, *Organometallics* **1989**, *8*, 363–368.

Received: June 18, 2009

Published Online: November 9, 2009